R Center in KCl; Stress Effects in Optical Absorption*

R. H. SILSBEE
Laboratory of Atomic and Solid State Physics and Department of Physics, Cornell University, Ithaca, New York
(Received 2 November 1964)

The R_2 optical absorption band in KCl shows a prominent zero-phonon line at liquid-helium temperature. This line may be split by application of uniaxial stress to the crystal, and the qualitative dependence of this splitting upon the direction of the stress and the polarization of the measuring light implies that the absorption is to be associated with a defect with a [111] axis of symmetry. The dependence of the intensities of the split components upon stress implies that the ground state is degenerate. The ground and low-lying excited states of van Doorn's F_3 model are discussed in terms of a continuum model for this center, as well as the implications of the Jahn-Teller effect which results from the coupling of these electronic states to the lattice vibrations. These considerations, in addition to being consistent with the results on the zero-phonon line, predict a stress-induced dichroism in all of those broad-band absorptions of the center which have transition moments in the plane of the triangle of F centers. An experimental study of the stress-induced dichroism has allowed the identification of six distinct transitions of the R center: a transition in the region of the N bands, one near the M band, the familiar R_1 and R_2 bands, a broad transition underlying the R_1 and F bands, and a narrow band on the violet side of the F band. The symmetry of the corresponding excited states is also obtained from the nature of the stress-induced dichroism. These experimental results are consistent with the qualitative predictions of the continuum F_3 model. These conclusions, supplemented by results on the spin quartet states of the R center and by polarized bleaching experiments, give the relative locations of ten distinct states of the R center.

I. INTRODUCTION

THE van Doorn model of the R center,[1,2] a cluster of three F centers, has received considerable experimental support including work on polarized luminescence,[1,3] polarized bleaching,[4] and radiation equilibria.[5,6] The observation of the zero-phonon line of the R_2 band[7,8] suggested that a study of the stress induced splitting of this line might give added support to that model. These studies did indeed confirm the F_3 model[9] but also led to a more detailed study of the center than had been anticipated. The ground state of the R center is degenerate and this degeneracy may be lifted by application of a uniaxial stress. The resultant preferential population of the lower state at low temperatures produces a marked anisotropy, or stress-induced dichroism, in the absorption spectrum of the stressed crystal. This stress-induced dichroism appears in many of the transitions associated with the R center and allows a simple identification of R-center transi ions without need for lengthy studies of changes in line shapes with different preparation methods, etc.

After a brief description of the experimental techniques in Sec. II, Sec. III describes the data on the splitting of the zero-phonon line and compares it with a simple phenomenological theory. Section IV gives a brief qualitative discussion of the electronic structure of the center and Sec. V introduces the interaction of the center with the lattice modes. In particular the need for a description in terms of the Jahn-Teller effect is discussed and then in Sec. VI a theoretical model is set up with which to describe the results of the stress-induced dichroism. Section VII presents the results of these experiments and relates the experiments to the models of Secs. IV and VI.

II. EXPERIMENTAL METHOD

The experimental techniques used in this experiment were quite conventional and require little discussion. The optical absorption data were obtained with a Cary Model 14 Spectrophotometer using a PbS detector for most of the studies, though for some work on the zero-phonon line the beam was brought out of the detector compartment with mirrors to a cooled RCA 7102 photomultiplier. The light was polarized by a Rochon prism in the entrance window of the spectrometer, a procedure which is more satisfactory than placing the polarizer in the sample chamber since the transmission of the Cary is not balanced for the two polarizations, showing large unbalances (Δ o.d. ~ 0.1) near the wavelengths at which higher order reflections reach grazing angles at the grating. The residual dichroism varied slowly with wavelength and from run to run but during runs rarely exceeded a difference in optical density of 0.03 for the two polarizations. These variations were not eliminated and in some instances limited the precision of the experiments.

The early work was carried out with a nested pair of simple slit silvered Dewars, the nitrogen bubbling

* Work supported in part by the U. S. Atomic Energy Commission and the Advanced Research Projects Agency.
[1] C. Z. van Doorn, Philips Res. Repts. **12**, 309 (1957), Suppl. #4 (1962).
[2] H. Pick, Z. Physik **159**, 69 (1960).
[3] W. D. Compton and C. C. Klick, Phys. Rev. **112**, 1620 (1958).
[4] F. Okamoto, Phys. Rev. **124**, 1090 (1961).
[5] S. Schnatterly and W. D. Compton, Phys. Rev. **135**, A227 (1964).
[6] See W. D. Compton and H. Rabin, *Solid State Physics* (Academic Press Inc., New York, to be published), Vol. 16, for an excellent review of the experimental results on the M and R centers.
[7] C. J. Delbecq and P. Pringsheim, J. Chem. Phys. **21**, 794 (1953).
[8] D. B. Fitchen, R. H. Silsbee, R. A. Fulton, and E. L. Wolf, Phys. Rev. Letters, **11**, 275 (1963).
[9] R. H. Silsbee, Bull. Am. Phys. Soc. **9**, 88, 211 (1964).

prevented by flowing helium gas through the liquid nitrogen above the optical path. Later an optical Dewar with flat windows and a nitrogen-temperature radiation shield with apertures for the light beam gave better performance. Liquid-hydrogen runs were performed in both Dewars flowing helium gas through the hydrogen to prevent boiling at the sample.

The stress was applied to the crystal via a cylinder, slotted to pass the light beam, and piston which were supported and driven by a pair of concentric thin wall stainless tubes leading out of the Dewar. The stress, which is thus perpendicular to the light beam, was applied in the early experiments by loading the piston with weights and later by means of a hydraulic pump and cylinder. The stress data did not reproduce well, numerical coefficients differing by as much as 40% between different runs. The source of this poor reproducibility, probably nonuniform strain in the sample, was not eliminated since the symmetry of the effects, not the magnitude, was the point of main concern.

The crystals were Harshaw, cleaved or ground, as appropriate, to dimensions roughly $3\times3\times15$ mm with the long axis of the crystal, the axis of uniaxial stress, parallel to either the 100, 110, or 111 crystallographic directions. For most of the runs the crystals were x-ray colored to F-center optical densities of 2 to 6 and then bleached under a fluorescent lamp to develop the R band to an optical density of 0.2 to 1 at 4.2°K. This bleaching time was about 10 min.

The polarized bleaching studies were carried out essentially as described by Okamoto[4] except that crystals were ground to have faces parallel to 111, 110, and 112 planes, convenient for bleaching with light polarized in the 111 direction, the most advantageous for the development of the R band.

The luminescence was measured using two Bausch and Lomb 250-mm grating monochromators one for defining the exciting wavelength, one to analyze the emission. The same Dewar was used as for the absorption measurements, with the exciting and emission beams at right angles. Filters were used to avoid higher order response of the monochromators. The analyzing monochromator and PbS detector were roughly calibrated for sensitivity by using a tungsten lamp as a black-body "standard." This is very necessary because of the sharply peaked monochromator response at approximately 1.2 μ.

III. STRESS-INDUCED SPLITTINGS OF THE R-CENTER ZERO-PHONON LINE

The application of uniaxial mechanical stress to a crystal showing a sharp optical transition may result in a splitting of that line into several components if the applied stress lowers the symmetry of the crystal. Several authors have shown how these stress-induced splittings relate to the microscopic symmetry of the center responsible for the transition observed.[10] The important information to obtain from the experiment is, for several orientations of the stress axis with respect to the crystallographic axes, the number of components and the relative intensity of each as measured with light polarized both perpendicular and parallel to the axis of the applied stress. Figures 1(a)–1(d) show results of such experiments carried out at liquid-hydrogen temperature for the R_2 zero-phonon line in KCl. Also shown are the line positions and relative intensities predicted by the phenomenological theory outlined below.

The R-center model proposed by van Doorn, Fig. 2(a), has C_{3v} symmetry and the states of that center will belong to representations E, A_1, or A_2 of that point group. Take as a model for the R_2 zero-phonon line a transition from a doubly degenerate ground state of E symmetry to an excited state of A_2 symmetry.

The effect of an applied stress is to shift both the ground and excited states and, if the strain reduces the site symmetry, to lift the degeneracy of the ground state. There are eight different equivalent orientations in the crystal for the R center as proposed by van Doorn corresponding to the eight (111) directions. Because none of the experiments discussed here distinguishes between the centers related by inversion of the axes, it is sufficient to consider only the four orientations (111), ($\bar{1}$11), (1$\bar{1}$1), (11$\bar{1}$). The properties of the ($\bar{1}\bar{1}\bar{1}$) center are identical to those of the (111) center, etc. Because the four types of centers are oriented differently with respect to the applied stress, the line splittings and shifts may be different for the originally equivalent centers.

The coupling of the ground state of the defect with the strain field in the crystal may be described by an effective Hamiltonian which, if only linear terms in the strain are considered, reduces to

$$\mathcal{H}^i=\mathbf{D}^i:\boldsymbol{\varepsilon}=\sum_{jk} D_{jk}{}^i\epsilon_{jk}. \tag{1}$$

i is an index which denotes the axis of the defect, (111), ($\bar{1}$11), etc., and $\boldsymbol{\varepsilon}$ is the macroscopic strain tensor

$$\epsilon_{jk}=\tfrac{1}{2}[(\partial u_j/\partial x_k)+(\partial u_k/\partial x_j)], \tag{2}$$

for a strain defined by a displacement function $\mathbf{u}(\mathbf{x})$. $\mathbf{D}$ is an operator defined in the space spanned by the degenerate pair of ground states and the components $D_{jk}{}^i$ are conveniently thought of as two by two matrices in a representation defined by a particular choice of these two basis states. The symmetry of the defect implies restrictions on the components of the D tensor, reducing the number of independent coefficients to four.

The natural axes in which to discuss the center with a (111) symmetry axis are those indicated in Fig. 2(b), where the circles, all in the xy plane, denote the posi-

[10] A. A. Kaplyanskii, Opt. i Spektroskopiya **16**, 602 (1964) [English transl.: Opt. Spectry. **16**, 329 (1964)]; A. L. Schawlow, A. H. Piskis and S. Sugano, Phys. Rev. **122**, 1469 (1961).

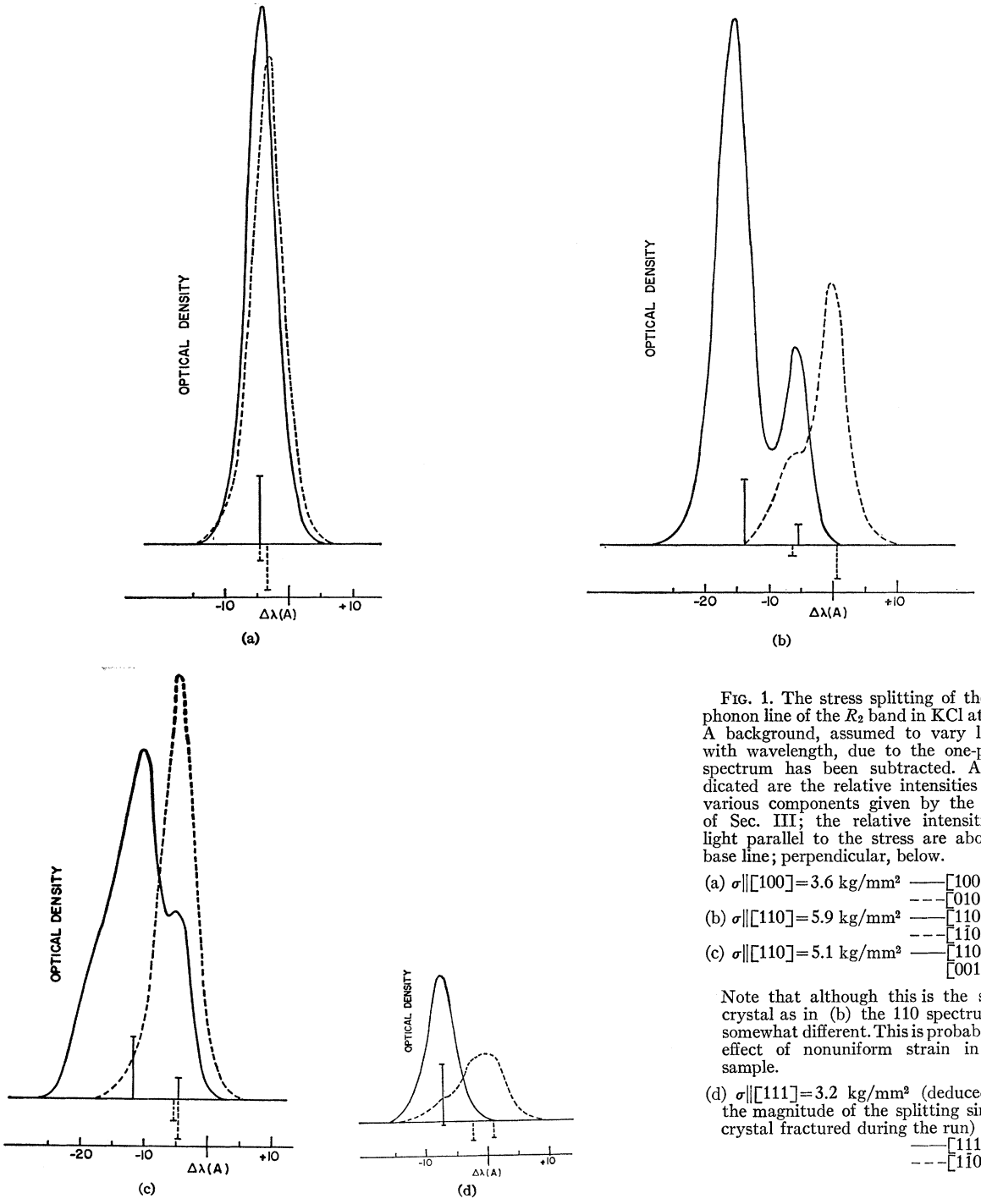

FIG. 1. The stress splitting of the zero-phonon line of the R_2 band in KCl at 20°K. A background, assumed to vary linearly with wavelength, due to the one-phonon spectrum has been subtracted. Also indicated are the relative intensities of the various components given by the theory of Sec. III; the relative intensities for light parallel to the stress are above the base line; perpendicular, below.

(a) $\sigma \| [100] = 3.6$ kg/mm² ——[100] light
---[010] light,

(b) $\sigma \| [110] = 5.9$ kg/mm² ——[110] light
---[1$\bar{1}$0] light,

(c) $\sigma \| [110] = 5.1$ kg/mm² ——[110] light
[001] light.

Note that although this is the same crystal as in (b) the 110 spectrum is somewhat different. This is probably an effect of nonuniform strain in the sample.

(d) $\sigma \| [111] = 3.2$ kg/mm² (deduced from the magnitude of the splitting since the crystal fractured during the run)
——[111] light
---[1$\bar{1}$0] light.

tions of the three negative ion vacancies; the directions of these coordinate axes with respect to the crystal cube axes are also given. Since the xz plane is a plane of symmetry for the defect it is convenient to choose as basis functions the states E_x and E_y which are even and odd, respectively, under reflection in this plane. If these functions are chosen to be real all of the elements of **D** will be real. The requirements that **D** be Hermitian and that its eigenvalues be the same for strains applied in directions equivalent under the symmetry operations of the crystal imply that in the (xyz) coordinate system of Fig. 2(b) the **D** tensor must

have the form

$$\mathbf{D}'=\begin{bmatrix}\begin{pmatrix}C+B & 0 & A\\ 0 & C-B & 0\\ A & 0 & -2C\end{pmatrix} & \begin{pmatrix}0 & -B & 0\\ -B & 0 & A\\ 0 & A & 0\end{pmatrix}\\ \begin{pmatrix}0 & -B & 0\\ -B & 0 & A\\ 0 & A & 0\end{pmatrix} & \begin{pmatrix}C-B & 0 & -A\\ 0 & C+B & 0\\ -A & 0 & -2C\end{pmatrix}\end{bmatrix}+T\mathbf{1}, \quad (3)$$

where the prime on $\mathbf{D}'$ indicates that $\mathbf{D}'$ is expressed in the local axes of Fig. 2(b). The 3×3 tensors operate in real space, the nine components corresponding to the choice of indices j and k of Eq. (1). The 2×2 structure operates in the space defined by the states E_x and E_y the upper left element corresponding to the E_y, E_y component of $\mathbf{D}$, etc. The unit tensor $\mathbf{1}$ is the direct product of the unit tensors of both spaces. To the extent that a continuum model of three F centers is valid, the center has reflection symmetry in the plane of the vacancies and hence has D_{3h} symmetry and not C_{3v}. Under the higher D_{3h} symmetry the coefficient A vanishes and one might therefore expect it to be small for the actual R center even though it is allowed by the C_{3v} symmetry.

The reduction of the coupling tensor to four constants can be argued as follows. The irreducible tensor components of strain transform in the following way

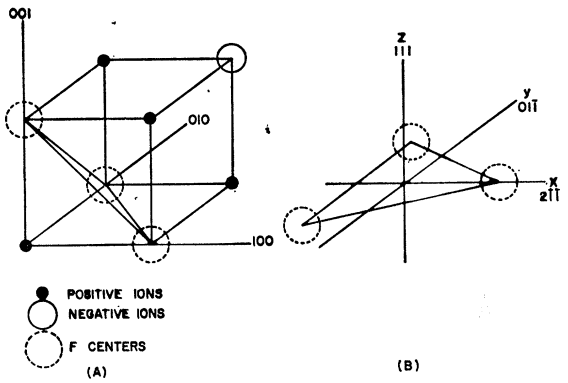

FIG. 2. Van Doorn's model of the R center. (a) Ionic configuration, (b) local axes for the (111) R center.

under the operations of C_{3v}: $(\epsilon_{xx}+\epsilon_{yy}+\epsilon_{zz})$ as A_1; $(\epsilon_{xx}+\epsilon_{yy}-2\epsilon_{zz})$ as A_1; $(\epsilon_{xx}-\epsilon_{yy})$ and $-\epsilon_{xy}$ as E; and ϵ_{xz} and ϵ_{yz} as E. The matrix elements of any one of these perturbations among the two states E_x and E_y are then specified by a single constant. The constants appropriate to the four tensor components in the order listed above are T, C, B, and A.

A rotation of axes from the xyz frame of Fig. 2(b) to the cube axes of the crystal gives for the coupling tensor of the (111) defect

$$\mathbf{D}^{(111)}=\tfrac{1}{3}\begin{bmatrix}\begin{pmatrix}2\sqrt{2}A+2B & & \\ (1/\sqrt{2})A-B-3C & -\sqrt{2}A-B & \\ (1/\sqrt{2})A-B-3C & -\sqrt{2}A+2B-3C & -\sqrt{2}A-B\end{pmatrix} & \begin{pmatrix} & & \\ & & \\ & & \end{pmatrix}\\ \begin{pmatrix}0 & & \\ (\sqrt{3}/\sqrt{2})A-\sqrt{3}B & \sqrt{6}A+\sqrt{3}B & \\ -(\sqrt{3}/\sqrt{2})A+\sqrt{3}B & 0 & -\sqrt{6}A-\sqrt{3}B\end{pmatrix} & \begin{pmatrix}-2\sqrt{2}A-2B & & \\ -(1/\sqrt{2})A+B-3C & \sqrt{2}A+B & \\ -(1/\sqrt{2})A+B-3C & \sqrt{2}A-2B-3C & \sqrt{2}A+B\end{pmatrix}\end{bmatrix}+T\mathbf{1}, \quad (4)$$

where the missing elements are given by the symmetry of D in both the three- and two-dimensional spaces. The D tensors for the other three orientations of defects may be obtained from (4) by appropriate change of sign of the components off diagonal in the real space indices. For the $(11\bar{1})$ defect, for example, the signs of the xz and yz components of $\mathbf{D}$ are changed.

For a given applied stress, ϵ_{ij}, the compliance coefficients, $S_{11}=2.12$, $S_{12}=-0.21$, $S_{44}=15.1\times10^{12}$ cm^2/dyn, give the macroscopic strain and the relations (4) give the Hamiltonian matrix of the ground state for this applied stress and for each of the four defect orientations. For the excited state the corresponding coupling tensor is only 3×3 since the state is nondegenerate. However, the experiment measures only the difference in energy of the ground and excited states. Since the coupling coefficients of the excited state enter the observed transition energies just as do the C and T coefficients of Eqs. (3) and (4), the experiment cannot distinguish the relative contributions of the two states to the line shift. It is convenient then to think of the excited state as being unaffected by the strain, and all of the shift as arising from shifts of the ground state and this point of view will be followed below. The C and T coefficients must ultimately be interpreted as the differences in the shifts of the ground and excited states produced by the corresponding strains; in contrast, the A and B relate to the splitting of the ground-state degeneracy and depend only upon the properties of the ground state.

Table I gives the results of such a calculation for the uniaxial stress applied along each of the directions (100), (110), and (111), the first column giving the energies of the various ground-state components which arise. An arbitrary direction of the applied stress would result in eight different components, but the greatest multiplicity developed for the stresses used here is four. The second column indicates the defect orientations that give the relative intensities of the various components with different polarizations of light as

TABLE I. Stress splittings of zero-phonon line.

Energies—add $(S_{11}+2S_{12})T$ to all entries in this column	Defect orientation	Relative intensities in light polarized as shown			Total intensity
σ along (100)		100	010	001	
$\frac{2}{3}\sigma(S_{11}-S_{12})(\sqrt{2}A+B)$ ↖	111, $\bar{1}11$,	8/3	2/3	2/3	4
$-\frac{2}{3}\sigma(S_{11}-S_{12})(\sqrt{2}A+B)$ ↗	$1\bar{1}1$, $11\bar{1}$	0	2	2	4
σ along (110)		110	$1\bar{1}0$	001	
$\frac{1}{3}\sigma\{-(S_{11}-S_{12})(\sqrt{2}A+B)-S_{44}(A/\sqrt{2}-B)-\frac{3}{2}S_{44}C\}$ ↖	111, $11\bar{1}$	2/3	0	4/3	2
$\frac{1}{3}\sigma\{-(S_{11}-S_{12})(\sqrt{2}A+B)+S_{44}(A/\sqrt{2}-B)-\frac{3}{2}S_{44}C\}$ ↗		0	2	0	2
$\frac{1}{3}\sigma\{-(S_{11}-S_{12})(\sqrt{2}A+B)+S_{44}(A/\sqrt{2}-B)+\frac{3}{2}S_{44}C\}$ ↙	$\bar{1}11$, $1\bar{1}1$	0	2/3	4/3	2
$\frac{1}{3}\sigma\{-(S_{11}-S_{12})(\sqrt{2}A+B)-S_{44}(A/\sqrt{2}-B)+\frac{3}{2}S_{44}C\}$ ↘		2	0	0	2
σ along (111)		111	$0\bar{1}1$	$\bar{2}11$	
$-\sigma S_{44}C$	111	0	1	1	2
$(\sigma/9)S_{44}(-2\sqrt{2}A+4B+3C)$ ↖	$\bar{1}11$, $1\bar{1}1$,	8/3	1/6	1/6	3
$(\sigma/9)S_{44}(2\sqrt{2}A-4B+3C)$ ↗	$11\bar{1}$	0	3/2	3/2	3

derived from dipole selection rules, using the eigenstates of the stress Hamiltonian and assuming the excited state to transform as A_2.

The intensities given in Table I would be the observed intensities if the two components of the ground state were equally populated. Because the ground-state splittings in these experiments are comparable with kT there is preferential population of the lower of the two ground-state components and an enhancement of the higher energy transitions. [The arrows in Table I indicate the states which are favored by this Boltzmann factor and which states are depopulated. The arrows can connect only pairs of energies which are associated with the same defect orientation.] The theoretical line intensities given in Fig. 1 include the factor resulting from this repopulation. The values and estimated accuracy of the constants chosen to give the results of Fig. 1 are $A=0.00\mp0.02$, $B=0.15\mp0.02$ and $C=0.12\mp0.02$ in the dimensionless units, fractional energy shift per unit strain. The value $T=0.75\mp0.1$, agrees with Fitchen's measurement of the shift with hydrostatic pressure. Note that the constant A is less that 15% of B and C, consistent with the guess that the departure of the symmetry from D_{3h} symmetry is small.

Although the model described had C_{3v} symmetry a number of different symmetry groups would have given similar results. The important features of the required symmetry are that the group must have a unique 111 symmetry axis and contain two as well as one dimensional representations. This requirement eliminates most defect models as candidates for the R center, including, at least in principle, the more highly symmetric tetrahedron of F centers which has four threefold axes. In practice, a strong static Jahn-Teller distortion of the F_4 model might fit the data but this occurrence seems unlikely since the tunneling frequency among the distortions would have to be less than 10^{-3} sec^{-1}, the inverse of the experimental times. The experimental results do not distinguish between A_1 and A_2 symmetry for the excited states, the assignment of A_2 symmetry for the excited state being based on results discussed later.

IV. ELECTRONIC STATES OF THE R CENTER

The results of the stress splitting experiment are in accord with the symmetry of the van Doorn model of the R center. This section develops this model qualitatively with the ultimate goal of supplying a theoretical framework in which to interpret other experimental results concerning the optical absorption of the R center.

The lowest states can be considered as arising from the perturbation of three isolated F centers, each in its ground state, by the overlap of the three electrons as the centers are brought closer together. When the centers are isolated the twofold spin degeneracy of each ground state implies that the ground state is $(2)^3=$ eightfold degenerate. As the intercenter distance is reduced the exchange energies lift that degeneracy and give two states, a spin quartet with no orbital degeneracy denoted by $^4A_1$ and an orbitally degenerate pair of spin doublets, ^2E, giving a total of 8 states. The metastable spin quartet, $^4A_1$, and similarly the higher spin quartet states are not of interest in this work because the transitions to these states from the spin doublet ground state are forbidden. Seidel *et al.*[11] have observed spin resonance in the metastable lowest spin quartet state in further confirmation of the F_3 model.

One may also get a qualitative picture of the excited states of the R center by noting the possible excited states of the three isolated centers. Since any of the eight degenerate ground states is connected to a distinct excited state by exciting an electron on any one of the three centers to any one of the three p functions on that center the total degeneracy of the first excited

[11] H. Seidel, D. Schmid, and M. Schwoerer, Z. Physik (to be published).

state is 72. It is straightforward to form linear combinations of these excited states which form basis sets for the various representations of the D_{3h} group, the symmetry group of the simplest continuum model of three vacancies. Twenty four of the 72 excited states correspond to excitation of an electron to a state which is odd in reflection in the plane of the triangle of vacancies, the remaining 48 are even under this reflection. The 24 odd states, denoted by the superscript °, can further be broken down into 2 spin quartet states, an orbitally nondegenerate $^4A_1°$ and an orbitally degenerate $^4E°$, accounting for 12 of the 24; and four spin doublets, $^2A_1°$, $^2A_2°$, and $^2E°$ taken twice, for the other 12. Of these six energy levels only the four spin doublets are of concern in the optical absorption experiments. The 48 even states break up in the same way giving four quartet levels and eight doublets.

As in the case of the lowest levels, this 72-fold degeneracy is lifted as the three centers are brought closer together. The overlaps will be least for the states odd in relection in the plane of the triangle and one might expect little splitting of these states and hence their optical absorption would be expected to lie in the region of the *F* band. The results of Okamoto's polarized bleaching experiments[3] indeed indicate transitions with moments in the *z* direction of Fig. 2(b) which lie in the *F* region. These would correspond to transitions to the two $^2E°$ states noted above which are odd in reflection in the plane of the triangle.

The states derived from excitations of one of the three *F* centers to a *p* state lying in the plane of the triangle will be appreciably altered by overlap and, if these states were the only ones involved, would lead to the even states indicated in Fig. 3, half of the 48

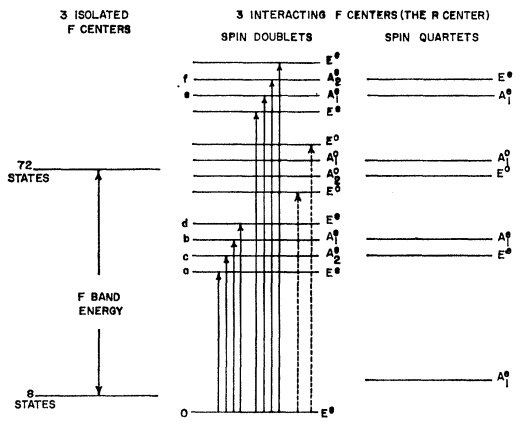

FIG. 3. A schematic representation of the energy-level structure of the *R* center. The letters to the left of the spin-doublet levels are used later to identify the states observed in the stress experiments. The ordering of the lowest five spin doublets and the lowest quartet is that given by the calculation of Hirschfelder; the ordering of the remaining levels is of little significance. Assuming D_{3h} symmetry, the solid lines give transitions allowed from the ground state for light polarized in the plane of the triangle of *F* centers; the dashed lines, the transitions allowed for light polarized perpendicular to that plane.

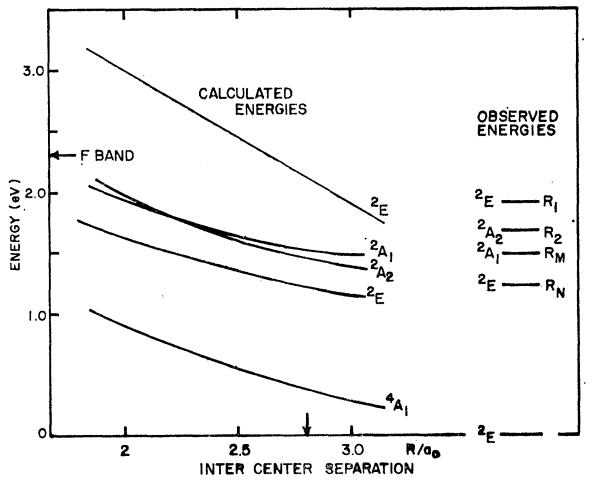

FIG. 4. Energies of the lower excited states of the *R* center, relative to the ground state, based on Hirschfelder's calculation for H_3 as a function of the *F*-center separation in units of the Bohr radius for the problem. Also indicated are estimates of the energies based upon the optical results discussed later as well as the inter-*F*-center separation in units of the Bohr radius as estimated from ENDOR results (Ref. 13) and Gourary and Adrian's (Ref. 14) type-*I* wave function. The vertical scale is adjusted to fit the *F*-band energy for an isolated *F* center in the same continuum model.

forming bonding states below the *F* energy and half-forming antibonding states above. This is a grossly oversimplified picture and one expects the energy-level structure to differ appreciably from this as a result of the admixture of states corresponding to electron transfer from one center to another, and some of the antibonding states indicated in Fig. 3 may well lie in or below the region of the *F* band. The main point to be made is that there should be a large number of optically accessible excited states of the center described by the van Doorn model and the R_1 and R_2 bands may represent only a small fraction of the observable transitions of the *R* center.

In Fig. 3 the selection rules from the ground state are indicated for the idealized continuum model with D_{3h} symmetry. None of the results of the experiments described below are of sufficient precision to detect the relaxation of the D_{3h} selection rules which would be implied by reducing the symmetry to C_{3v}, the actual symmetry group of the van Doorn model. Hence, for simplicity, D_{3h} symmetry will be assumed for most of the arguments in the rest of this paper.

The ordering of the four lowest excited spin doublets in Fig. 3 is based on the calculation of Hirschfelder[12] for the H_3 molecule, the relative positions of the remaining states having no particular significance except for placing of the odd symmetry states in the general region of the *F* excited state energy and the antibonding even states above these. Hirschfelder's linear-combination-of-atomic-orbitals calculations, using only *s* functions on the individual centers but including

[12] J. O. Hirschfelder, J. Chem. Phys. 6, 795 (1938).

ionic configurations, have been extended slightly to calculate the energies of these four lowest excited spin doublets with respect to the ground state and the results, using 4/3 times the F-excitation energy as the unit of energy, are given in Fig. 4, as a function of the vacancy separation in units of the effective Bohr radius. Also indicated is the value of R, assuming the vacancies to lie on normal lattice sites, using an estimate from electron-nuclear-double-resonance (ENDOR) experiments[13] and from Gourary and Adrian[14] for the effective Bohr radius. Finally the energies on the right-hand side are estimates of the energies and symmetries of various excited states of the R center as deduced from the experimental results described later. Since only single center s functions were used in this calculation one should expect no more than the qualitative agreement which is apparent.

The next step in calculating the electron energy levels in the static lattice would be to consider the splittings of the ^2E levels by the spin-orbit interaction. There is considerable evidence, from both optical- and spin-resonance[15] experiments, that the coupling with the lattice vibrations gives splittings by the Jahn-Teller effect which effectively quench, or at least greatly reduce, the orbital moment. Hence the next section treats the effects of the vibrational coupling, leaving the effect of the spin-orbit coupling to be treated in a later publication concerned primarily with the spin-resonance properties of the R center.

V. VIBRONIC STATES OF THE R CENTER

The orbital degeneracy of the ^2E electronic ground state of the F_3 model and of a number of the excited states imply the possibility of a Jahn-Teller effect. Distortions of E symmetry will lift the degeneracy of these electronic states and the minimum in the potential energy of the full crystal will correspond to some finite distortion in these modes. In the presence of a Jahn-Teller effect the vibronic wave functions are no longer simple products of electronic and vibrational parts. As a consequence the vibrational coupling not only broadens the transitions but also significantly alters the broad-band selection rules from those of the starting electronic states.

Again, as in the brief discussion of the electronic structure, the aim of this section is to give the minimum theoretical framework required to understand qualitatively the experiments but not to give a complete theoretical picture. The lattice modes will be represented schematically by the three coordinates indicated in Fig. 5. The first, a breathing mode, has A_1 symmetry and contributes to the optical line breadth according to the usual theory of the broadening of optical transitions.

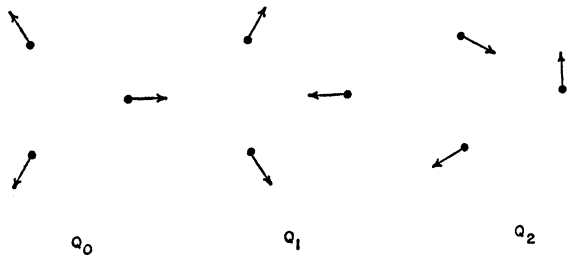

FIG. 5. Normal vibrational modes of a triatomic molecule.

Its effect will be included only when specifically necessary. The second and third modes are of E symmetry and will be degenerate in frequency. It is these modes which contribute to the Jahn-Teller effect and this section will primarily discuss the consequences of that coupling.

Since the three "force centers" in this problem are ion vacancies, the modes of Fig. 5 are at first sight meaningless. What is meant by this model is the following. In principle one could perform a normal mode analysis of a crystal containing a single R center, the effect of the coupling to the three electrons in the R center being omitted for the time being. These modes could then be classified by their symmetry character under the symmetry operations of the R center. Many of these modes would be of A_1 symmetry and in the model of this discussion, the effect of all of these modes is represented by a single breathing mode, Q_0. Most qualitative predictions concerning line broadening, Stoke's shift, etc., are unaltered by this apparently gross approximation if the frequency of this effective mode is an appropriately weighted average of the frequencies of the actual modes. The situation with the modes of A_2 symmetry is similar and since the effects of these modes are qualitatively similar to those of the A_1 modes the effect of the A_2 modes will be included with the A_1 coordinate. There is no intention in this discussion to imply either the existence or absence of any localized modes of these symmetry types at the R center. The qualitative discussion is independent of any such considerations.

The situation with the modes of E symmetry which contribute to the Jahn-Teller effect is more complex. Suppose there is no localized mode in the absence of coupling to the electronic states of the defect. With the coupling a significant Jahn-Teller distortion may arise only through a cooperative effect among the modes of E symmetry, since the strength of coupling to the individual modes is only of order $1/N$. Slonczewski[16] has discussed this problem in certain models for the lattice modes and has shown the existence, in these models, of a pair of collective modes. Recognizing that the justification of such a procedure is open to some question, it has still seemed fruitful to examine the con-

[13] M. Schwoerer and H. C. Wolf, Z. Physik **175**, 457 (1963).
[14] B. S. Gourary and F. J. Adrain, *Solid State Physics* (Academic Press Inc., New York, 1960), Vol. 10, p. 128.
[15] D. C. Krupka and R. H. Silsbee, Phys. Rev. Letters **12**, 193 (1964).
[16] J. C. Slonczewski, Phys. Rev. **131**, 1596 (1963).

sequences of the simple model in which, just as for the modes of A symmetry, a single pair of E modes is taken to represent the effect of all the modes of this symmetry. If localized modes in the usual sense exist and are of E symmetry, the coordinate Q_1 and Q_2 are taken to be of these modes.

This model is essentially that discussed by Longuet-Higgins, Öpik, Pryce, and Sack[17] (LHOPS), and the remainder of this section draws heavily upon that paper. In the absence of the coupling to the electronic state, the potential energy surface for the two modes Q_1 and Q_2 may be represented as a paraboloid of revolution. If polar coordinates are introduced in the Q_1, Q_2 coordinate space

$$\begin{aligned} Q_1&=r\cos\phi\,,\\ Q_2&=r\sin\phi\,, \end{aligned} \tag{5}$$

then the potential energy for these modes is $V(r)\sim\frac{1}{2}r^2$ in the units of LHOPS and the solution of the vibrational problem may be written as

$$\begin{aligned} &\Psi_{nm}(r,\phi)=\rho_{nm}(r)e^{im\phi}\,,\\ &\quad E_{nm}=n\,,\\ &\qquad n=1,2\cdots\quad m=n-1,\,n-3,\,\cdots-n+1\,, \end{aligned} \tag{6}$$

where the units of energy are $h\omega$ if ω is the frequency of the E modes.

If the electron-lattice coupling is included, the electron degeneracy is lifted in first order by the Q_1 and Q_2 distortions and the parabolic potential surface splits, in first order, into the two-sheeted surface of Fig. 6, the surface being generated by a rotation of that figure about the vertical axis. The strength of the vibrational coupling is described by a parameter k such that the lowering of the potential minimum by this interaction is $k^2/2$, again in energy units $h\omega$. The solution of the full Schrödinger equation is more complex than the simple Born-Oppenheimer approach because, for small r, the electronic frequency associated with the difference in energy of the two branches of the potential surface is comparable with the vibrational frequencies.

The eigenfunctions of this problem, given by LHOPS, may be written

$$\begin{aligned} \Psi_{xpl}{}^i=\mu_{pl}{}^i(-r)\,&\cos l\phi[\mathcal{E}_x{}^i\cos(\phi/2)+\mathcal{E}_y{}^i\sin(\phi/2)]\\ &+(-)^{l-\frac{1}{2}}\mu_{pl}{}^i(r)\sin l\phi\\ &\times[\mathcal{E}_y{}^i\cos(\phi/2)-\mathcal{E}_x{}^i\sin(\phi/2)],\\ \Psi_{ypl}{}^i=\mu_{pl}{}^i(-r)\,&\sin l\phi[\mathcal{E}_x{}^i\cos(\phi/2)+\mathcal{E}_y{}^i\sin(\phi/2)]\\ &+(-)^{l-\frac{1}{2}}\mu_{pl}{}^i(r)\cos l\phi\\ &\times[\mathcal{E}_y{}^i\cos(\phi/2)-\mathcal{E}_x{}^i\sin(\phi/2)]. \end{aligned} \tag{7}$$

$\mathcal{E}_x{}^i$ and $\mathcal{E}_y{}^i$ are the pair of degenerate electronic wave functions, the $\mathcal{E}_x$ and $\mathcal{E}_y$ being even and odd under reflection in the xz plane of Fig. 2, the superscript i referring to the ground (0) or an excited (a or d) state

[17] H. C. Longuet-Higgins, U. Öpik, M. H. L. Pryce, and R. A. Sack, Proc. Roy. Soc. (London) **244**, 1 (1958).

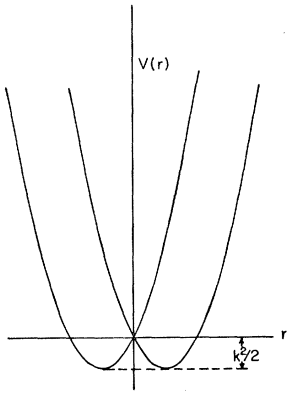

FIG. 6. The adiabatic potential for vibrational motion in the presence of a Jahn-Teller effect.

of E symmetry. The μ_{pl} (r) are radial wave functions discussed by LHOPS. The quantum numbers needed to specify completely the vibronic state are the electronic state i, the symmetry of the over-all state under reflection in the xz plane of Fig. 2(b) specified by x or y, a radial quantum number p which, for large static distortions, describes the excitation of radial vibrations across the trough of Fig. 6, and a half-integral azimuthal quantum number l which describes the rotational motion of the system around the trough of Fig. 6. The quantum numbers p take on the values 1, 2, 3, $\cdots$ and l the values of $\frac{1}{2}$, $\frac{3}{2}$, $\frac{5}{2}$, $\cdots$.

Because the vibrational modes of E symmetry cannot couple linearly to the electronic states of A_1 or A_2 symmetry, the vibronic wave functions for these states are written as the usual product functions,

$$\begin{aligned} \Phi_{xnm}{}^i&=\mathfrak{A}_1{}^i\sqrt{2}\rho_{nm}{}^i(r)\cos m\phi\,,\\ \Phi_{ynm}{}^i&=\mathfrak{A}_1{}^i\sqrt{2}\rho_{nm}{}^i(r)\sin m\phi\,,\\ \Phi_{xnm}{}^i&=\mathfrak{A}_2{}^i\sqrt{2}\rho_{nm}{}^i(r)\sin m\phi\,,\\ \Phi_{ynm}{}^i&=\mathfrak{A}_2{}^i\sqrt{2}\rho_{nm}{}^i(r)\cos m\phi\,, \end{aligned} \tag{8}$$

where the normalization constant $\sqrt{2}$ is replaced by unity for $m=0$, $\mathfrak{A}_1{}^i$ or $\mathfrak{A}_2{}^i$ are the electronic-state wave functions and the superscripts i on Φ and ρ refer to the electronic state from which these vibronic states are derived. In later discussions of the optical absorption among these various states it is convenient to remember the symmetry of the states as indicated below:

$$\begin{aligned} &\Psi_{xpl}{}^i \text{ and } \Psi_{ypl}{}^i \text{ transform as } E \text{ for}\\ &\qquad l=\tfrac{1}{2},\,\tfrac{5}{2},\,\tfrac{7}{2},\,11/2,\,\cdots,\\ &\Psi_{xpl}{}^i \text{ and } \Psi_{ypl}{}^i \text{ transform as } A_1 \text{ and } A_2,\\ &\qquad \text{respectively, for } l=\tfrac{3}{2},\,\tfrac{9}{2},\,15/2,\,\cdots,\\ &\Phi_{xnm}{}^i \text{ and } \Phi_{ynm}{}^i \text{ transform as } E \text{ for}\\ &\qquad m=1,\,2,\,4,\,5,\,6,\,\cdots,\\ &\Phi_{xnm}{}^i \text{ and } \Phi_{ynm}{}^i \text{ transform as } A_1 \text{ and } A_2,\\ &\qquad \text{respectively, for } m=0,\,3,\,6,\,\cdots. \end{aligned} \tag{9}$$

The discussion above is complete only if terms beyond linear in the electronic vibrational coupling are neg-

lected. The inclusion of quadratic terms in the electron lattice coupling or cubic terms in the lattice potential energy removes the axial symmetry of the potential of Fig. 6, giving 3 mimima in the potential trough. This trigonal potential lifts the degeneracy of the A_1 and A_2 vibronic states associated with the $l=\frac{3}{2}$, $\frac{9}{2}$, 15/2, $\cdots$ values and results in admixtures of states which differ by 3 in l value.[18] If both the linear and quadratic Jahn-Teller coupling terms are large, these three minima are deep compared with the vibrational energy and a good approximation to the lowest lying states is the static distortion corresponding to any of these three wells. This situation is frequently the case in systems showing the Jahn-Teller effect and corresponds to the trigonal potential lowering the energy of the lowest A_1 state of $l=\frac{3}{2}$ to nearly that of the lowest $l=\frac{1}{2}$ states. The energy difference between the $l=\frac{3}{2}$, A_1 state and the pair of $l=\frac{1}{2}$, E states is $\frac{3}{2}$ times the tunneling frequency of the system among the three wells. Reference 18 gives several energy-level diagrams for different limiting cases of the linear and quadratic couplings.

The consistency of the optical experiments with the model assuming an E ground state shows that such a strong localization does not exist for the R center. Straightforward calculations show that the results would be qualitatively different if this E-A_1 splitting or tunneling frequency were small compared with the splitting produced by the applied stress in these experiments. Furthermore, if this E-A_1 splitting were less than ~ 15 cm^{-1} but more than the zero-phonon linewidth (≈ 6 cm^{-1}) one would expect to see effects of thermal population of the A_1 state with increasing temperature. The absence of such effects implies that this A_1 state is at least 20 cm^{-1} above the ground state. This observation also places a limit on the strength of the linear coupling in the ground state since a strong linear coupling even in absence of the quadratic term brings the $l=\frac{3}{2}$ states close to the $l=\frac{1}{2}$ states. These arguments suggest that the parameter k^2 of LHOPS is less than 7 for the R-center ground state.

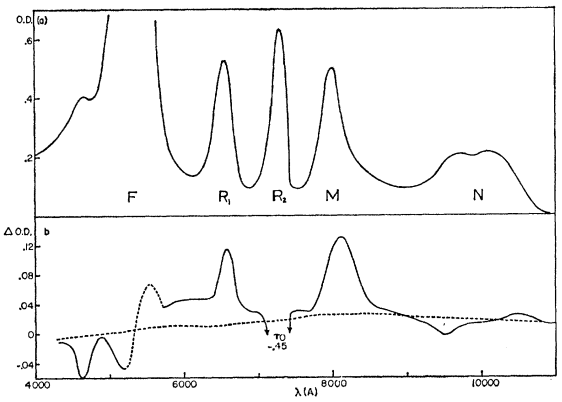

FIG. 7. (a) The absorption spectrum of KCl containing aggregate centers at 2°K. The step in the base line in the region of the N band does not normally appear (e.g., see Fig. 11) and is not related to the R center. (b) The difference spectrum, [1$\bar{1}$0]−[110] with a [110] stress of 2.5 kg/mm^2. The dashed curve is an estimate of the residual dichroism at zero stress.

[18] M. S. Child and H. C. Longuet-Higgins, Phil. Trans. Roy. Soc. 254, 259 (1961).

In terms of the states described in this and the previous section, the zero-phonon line is consistently interpreted as an excitation from the degenerate pair of states $\Psi_{x1\frac{1}{2}}{}^0$ and $\Psi_{y1\frac{1}{2}}{}^0$ to one of the states $\Phi_{x10}{}^b$ or $\Phi_{y10}{}^c$, the choice depending on whether the R_2 excitation is to the A_1 or A_2 electronic state of Fig. 4. The Jahn-Teller effect is weak, corresponding to a $k^2 \lesssim 7$ since at temperatures as high as 20°K there is no evidence for thermal excitation to higher vibronic states. Similarly the quadratic Jahn-Teller coupling and the third-order elastic terms are sufficiently weak that there is not a strong stabilization of the three static distortions of the defect.

VI. THEORY OF BROAD-BAND DICHROISM

The presence of a different integrated absorption intensity of the zero-phonon line for different polarizations of light has already been explained in terms of the stress splitting of the ground state of the system and the preferential population of the lower of these two states. This resultant stress induced anisotropy of the crystal is echoed in a number of absorption bands as indicated in Fig. 7. This section develops the qualitative implications of the theory developed by LHOPS and the following section compares these predictions with the results of Fig. 7.

For simplicity of argument, consider the center with the orientation of Fig. 2(b) with the E_x, E_y degeneracy lifted by a stress applied along the x axis leaving the E_y state low and the only state thermally populated. The problem is to determine the effect of this strain splitting on the absorption of light propagating in the z direction and polarized either in the x or y directions. In the experiment the light does not propagate perpendicular to the plane of the triangle and at first sight the following results would need modification. To the extent that the R center has D_{3h} symmetry, the transitions discussed here are induced only by that component of the optical field which lies in the plane of the triangle. With this assumption the results of the predictions below are applicable to the experimental results. In C_{3v} symmetry, the E-E transitions would also be partially allowed in light polarized in the z directions and the predictions below would have to be modified. This modification has not been included and is felt to be unimportant.

The intensity of the transition from the ground state $\Psi_{y1\frac{1}{2}}{}^0$ to an excited state $\Psi_{x(\text{or } y)pl}{}^i$ or $\Phi_{x(\text{or } y)nm}{}^i$ will be given by the square of a transition matrix element which has the form,

$$M_{x(\text{or } y)pl;\ y}{}^{i0} = \int \Psi_{x(\text{or } y)pl}{}^i \mathcal{H}' \Psi_{y1\frac{1}{2}}{}^0 dq\, r dr d\phi. \quad (10)$$

$\int dq$ is over electronic coordinates and $\int r dr d\phi$ is the integral over the two normal coordinates Q_1 and Q_2; $\mathcal{H}'$ describes the interaction of the electron with the electric field of the optical wave.

The electron matrix elements are computed first and are assumed (Condon approximation) not to depend on the nuclear coordinates except as directly implied by the form of the wave functions of Eq. (7). A single parameter g_i is introduced as the magnitude of the electronic matrix element of an allowed electronic transition from the ground to the one of the excited states i. The transition elements between suitably chosen states are then either $\pm g_i$ or zero depending on the symmetry of the two states. For an $E \rightarrow E$ transitions, for instance, one has

$$-(\mathcal{E}_x{}^i|\mathcal{H}'_x|\mathcal{E}_x{}^0)=(\mathcal{E}_y{}^i|\mathcal{H}_x'|\mathcal{E}_y{}^0)=(\mathcal{E}_y{}^i|\mathcal{H}_y'|\mathcal{E}_x{}^0)$$
$$=(\mathcal{E}_x{}^i|\mathcal{H}_y'|\mathcal{E}_y{}^0)=g_i,$$
$$(\mathcal{E}_x{}^i|\mathcal{H}_y'|\mathcal{E}_x{}^0)=(\mathcal{E}_y{}^i|\mathcal{H}_y'|\mathcal{E}_y{}^0)=(\mathcal{E}_y{}^i|\mathcal{H}_x'|\mathcal{E}_x{}^0)$$
$$=(\mathcal{E}_x{}^i|\mathcal{H}_x'|\mathcal{E}_y{}^0)=0, \quad (11)$$

where $\mathcal{H}_{x(\text{or } y)}'$ is the interaction Hamiltonian for light polarized in the x or y directions. Evaluation of the integral over ϕ gives the results of Table II.

Note that the angular integrations allow transitions only to vibronic states derived from E electronic states with l values $\frac{1}{2}$ or $\frac{3}{2}$, and to vibronic states derived from A electronic states (referred to below as A derived states) with m values of 0 or 1. These selection rules are a result of the assumption of full cylindrical symmetry which is implied by the neglect of higher than linear terms in the electronic-vibrational coupling. It will soon be clear that this assumption is not warranted.

TABLE II. Matrix elements from degenerate ground states.

Final electronic state symmetry	Final	Initial light	$\Psi_{y1\frac{1}{2}}{}^0$ x	$\Psi_{y1\frac{1}{2}}{}^0$ y	$\Psi_{x1\frac{1}{2}}{}^0$ x	$\Psi_{x1\frac{1}{2}}{}^0$ y
E	$\Psi_{yp\frac{1}{2}}{}^i$	E	$G_{1/2}{}^i$	0	0	$G_{1/2}{}^i$
	$\Psi_{xp\frac{1}{2}}{}^i$		0	$G_{1/2}{}^i$	$-G_{1/2}{}^i$	0
	$\Psi_{yp\frac{3}{2}}{}^i$	A_2	$G_{3/2}{}^i$	0	0	$G_{3/2}{}^i$
	$\Psi_{xp\frac{3}{2}}{}^i$	A_1	0	$G_{3/2}{}^i$	$G_{3/2}{}^i$	0
A_2	$\Phi_{yn0}{}^i$	A_2	$G_0{}^i$	0	0	$-G_0{}^i$
	$\Phi_{yn1}{}^i$	E	$G_1{}^i$	0	0	$G_1{}^i$
	$\Phi_{xn1}{}^i$		0	$G_1{}^i$	$-G_1{}^i$	0
A_1	$\Phi_{xn0}{}^i$	A_2	0	$G_0{}^i$	$G_0{}^i$	0
	$\Phi_{yn1}{}^i$	E	$G_1{}^i$	0	0	$G_1{}^i$
	$\Phi_{xn1}{}^i$		0	$G_1{}^i$	$-G_1{}^i$	0

$$G_0{}^i=g_i\int\rho_{n0}{}^i(r)[\mu_{1\frac{1}{2}}{}^0(-r)+\mu_{1\frac{1}{2}}{}^0(r)]rdr$$

$$G_1{}^i=\left(\frac{g_i}{\sqrt{2}}\right)\int\rho_{ni}{}^i(r)[\mu_{1\frac{1}{2}}{}^0(-r)-\mu_{1\frac{1}{2}}{}^0(r)]rdr$$

$$G_{\frac{1}{2}}{}^i=\tfrac{1}{8}g_i\int[\mu_{p\frac{1}{2}}{}^i(-r)+\mu_{p\frac{1}{2}}{}^i(r)][\mu_{1\frac{1}{2}}{}^0(-r)+\mu_{1\frac{1}{2}}{}^0(r)]rdr$$

$$G_{\frac{3}{2}}{}^i=\tfrac{1}{8}g_i\int[\mu_{p\frac{3}{2}}{}^i(-r)-\mu_{p\frac{3}{2}}{}^i(r)][\mu_{1\frac{1}{2}}{}^0(-r)-\mu_{1\frac{1}{2}}{}^0(r)]rdr$$

The dichroism induced by applied stress in the transitions from electronic E to A states and E to E states is markedly different. If only the lowest state, $\Psi_{y1\frac{1}{2}}{}^0$, is occupied then in the transitions to A_2 derived vibronic states x light can couple to both the $m=0$ and $m=1$ states but y light can couple only to the $m=1$ states. Since the intensity of both the x and y induced transitions to the $m=1$ states is the same, the absorption in x light will be greater than that in y light by just the contribution of the transitions to the $m=0$ states. Further it should be noted that, since for $m=0$ states, $n=$ odd and for $m=1$ states n is even, in y light one observes transitions involving the cooperation of an odd number of E mode vibrational quanta while in the difference spectrum, x light minus y light, one observes the intensity associated with the excitation of zero or an even number of E-mode quanta.

Some limit on the magnitude of the Jahn-Teller effect may also be crudely estimated from the strength of the dichroism. As discussed in LHOPS, the qualitative behavior of the radial function $\mu_{1\frac{1}{2}}{}^0(r)$ depends on the strength of the coupling parameter k^2. For strong coupling $\mu(r)$, representing the probability of finding the electron in the more favorable electronic state for a given distortion, is large near the value of r for which the potential of Fig. 6 is a minimum, and $\mu(-r)$ is very small. In this case the overlap integrals of Table II will vary moderately smoothly with n, showing no marked alternation going from even to odd n. If the variation with n is sufficiently smooth (the important values of n for this system are not large enough for this to be a good assumption) one then predicts for the ratio of integrated absorption strengths in x and y light of $(1+\frac{1}{2}):\frac{1}{2}$ or 3:1.

On the other hand, if the Jahn-Teller distortion is small, $\mu(-r)$ becomes comparable with $\mu(r)$ and in the limit $k^2=0$, $\mu(r)=\mu(-r)$. In this case the two terms in the overlap integral to the $m=1$ states almost cancel, the transition strength in y light decreases, and the ratio of integrated absorption strengths becomes greater than 3:1. In either case, for the R center, absorption bands to excited states derived from either A_1 or A_2 electronic states should be characterized by a strong dichroism, at least 3:1, in the limit of large stress and low temperature.

The situation for the transition to the bands associated with E electronic states is markedly different. First, since the excited E state is presumably also split by a Jahn-Teller effect and since the system is in an initially distorted state, excitation may occur to either of the sheets of the Jahn-Teller potential surface of the excited E state and a doublet band is expected if broadening by other modes is not excessive.

Second, the dichroism produced in the bands associated with the excited E states is much less marked than in the A derived bands. A brief inspection of Table II shows that for every transition in x light there is a corresponding transition of equal intensity in y light. The only mechanism for developing dichroism

in this model is simply the strain splitting of the various vibronic states. A straightforward calculation of the strain splitting of these excited states gives

$$l=\tfrac{1}{2};\ \Delta^i(\epsilon)=\tfrac{1}{2}[(\mathcal{E}_x{}^i|\mathcal{H}_\epsilon|\mathcal{E}_x{}^i)^2-(\mathcal{E}_y{}^i|\mathcal{H}_{\epsilon y}{}^i|\mathcal{E}_y{}^i)^2]\times[1-\int\mu_{pl}{}^i(-r)\mu_{pl}{}^i(r)rdr],$$
$$l=\tfrac{3}{2};\ \Delta^i(\epsilon)=0, \qquad (12)$$

where the matrix elements are the pure electronic matrix elements of the perturbing potential produced by the applied stress. It is these splittings $\Delta^0(\mathcal{E})$ for the ground state which are measured by the stress splitting experiments discussed in Sec. III. Thus the splitting of the excited $l=\frac{1}{2}$ states by the applied stress can result in a dichroism which would appear in a plot of x minus y absorption as the derivative of the band shape associated with the $l=\frac{1}{2}$ transitions.

Another source of dichroism results from removing the restriction of full cylindrical symmetry. The equality of the matrix elements to the A_1 and A_2 vibronic states derived from the E electronic state is a consequence of the assumed cylindrical symmetry and is not implied by the symmetry C_{3v}. Child and Longuet-Higgins[18] discuss briefly the effect of including the quadratic Jahn-Teller term and note that it reduces the symmetry of the resultant model Hamiltonian. One important consequence is to lift the degeneracy of the A_1 and A_2 ($l=\frac{3}{2}$) vibronic states and this will result in a dichroism, similar to that resulting from the strain splitting of the $E(l=\frac{1}{2})$ states, which will appear as a derivative in a dichroic spectrum. A second consequence of a quadratic Jahn-Teller term or third-order elastic term, referred to below as the trigonal potential since these terms introduce three depressions in the trough of Fig. 6, is to change the relative oscillator strength of the transitions to the A_1 and A_2 vibronic states.

At least two mechanisms contribute to this effect of the trigonal potential on the A_1 and A_2 transition probabilities. First, but probably not important for this problem, the trigonal term in the Hamiltonian will admix the A_1 and A_2 vibronic states derived from the E electronic states with the A_1 vibronic states of the A_1 electronic level and the A_2 states of the A_2 level. The oscillator strength of the resultant states is determined both by the degree of admixture and by the oscillator strengths of the $E^\circ\rightarrow A_1$ and $E^\circ\rightarrow A_2$ electronic transitions. Both of these factors will be different for the A_1 and A_2 vibronic mixture states and a dichroism will result.

More important for the problem at hand is the coupling by the trigonal potential among the levels of the ground state. In particular the ground state with stress, $\Psi_{yl\frac{1}{2}}{}^0$, will have admixed, in first order in the trigonal potential, an amount of the states $\Psi_{yp\frac{5}{2}}{}^0$ of order $V_3/\Delta E$. Here, if $k^2<5$, ΔE is of the order of $\hbar\omega$ and V_3 is the matrix element of the trigonal potential between the $l=\frac{1}{2}$ and $l=\frac{5}{2}$ states. This admixture will not affect the moment to the E derived $l=\frac{1}{2}$ states in first order, but since optical matrix elements exist from both the $l=\frac{5}{2}$ and $l=\frac{1}{2}$ components of the ground-state wave function to the excited $l=\frac{3}{2}$ states, the oscillator strengths to the A_1 and A_2 vibronic states are altered by the interference between the two parts of the matrix element. Ignoring coupling to all but the lowest $l=\frac{5}{2}$ vibronic state in the ground electronic system, the matrix elements for transitions from the ground state of E_y symmetry to the excited E-derived vibronic states of A_1 and A_2 symmetry are

$$M\sim\int_0^\infty rdr\{[\mu_{p\frac{3}{2}}{}^i(-r)-\mu_{p\frac{3}{2}}{}^i(r)]\times[\mu_{1\frac{1}{2}}{}^0(-r)-\mu_{1\frac{1}{2}}{}^0(r)]\pm(V_3\Delta/E)[\mu_{p\frac{3}{2}}{}^i(-r)+\mu_{p\frac{3}{2}}{}^i(r)]\times[\mu_{1\frac{1}{2}}{}^0(-r)+\mu_{1\frac{1}{2}}{}^0(r)]. \qquad (13)$$

The upper sign corresponds to the transition to the A_1 state with y light, the lower sign to the A_2 state with x light. This gives a dichroism, of strength proportional to the trigonal potential, which is believed to be the dominant effect in the dichroism of the transition to the E states. It should be noted that although the trigonal potential will mix together many states in both the ground and excited vibronic systems, the term of Eq. (13) gives the only first-order effect of this mixing by the trigonal potential except for the trivial generalization of including the coupling to the higher series of $l=\frac{5}{2}$ states, $\Psi_{yp'\frac{5}{2}}$.

One final important qualitative feature of this mechanism is the relative sign of the dichroism to be expected in the two bands associated with the E to E transition. As noted earlier, for a moderately strong Jahn-Teller effect ($k^2\approx1$) the function $\mu_{p\frac{1}{2}}(r)$ for the low-lying levels is large for positive and small for negative r, and in Eq. (13) the transition strength to the lower energy band or the lower sheet of the potential surface is dominated by the overlap of the $\mu_{p\frac{3}{2}}{}^i(r)$ function onto the ground-state function. The transition strength to the upper sheet, however, is determined by the overlap of $\mu_{p\frac{3}{2}}{}^i(-r)$ and a brief inspection of Eq. (13) shows that the interference term in the square of the matrix element will be of opposite sign for the two band components of the $E\rightarrow E$ transition.

In summary the optical bands associated with the $E\rightarrow A$ electronic transitions should show a strong stress induced dichroism at temperatures low enough to establish perferential population of the lower of the stress-split ground states. The $E\rightarrow E$ transitions will show a weak dichroism, the dominant effect in the experiments described below resulting from the effects of the quadratic Jahn-Teller coupling or cubic lattice energy terms. The magnitude of the dichroism and the relative sign in different regions of the spectrum may then be used to identify the symmetry of the excited states of the R center which give rise to the various optical absorption bands of that center.

VII. BROAD-BAND TRANSITIONS OF THE *R* CENTER

The extreme sensitivity of the *R*-center spectrum to stress results from the presence of a degenerate ground state. Since an orbital ground-state degeneracy is expected only for centers with high symmetry (at least a three- or fourfold symmetry axis), and then only for appropriate ground-state electronic configurations, the number of defect centers showing a strong stress-induced dichroism should be small. The basic hypothesis in these experiments was to assume that any stress induced dichroism implied the existence of an *R*-center transition in the corresponding region of the spectrum. A first check of this hypothesis is to compare the dichroism induced by stress at liquid-nitrogen temperature with that at 2°K. A marked reduction of the strength of dichroism at the higher temperature implies that the dichroism results, in part at least, from the preferential population of the lower level of a strain split ground state. Temperature insensitive dichroism implies the strain splitting of an excited state, or the shifts of the transition energies of low symmetry centers with nondegenerate states which depend upon the orientation of the center with respect to the stress axis. Use of this technique showed that within the precision of the subtraction procedures the dichroism in the region of the *F* band in Fig. 7 results from a stress-induced splitting of the excited state of the *F* center. In the rest of the spectrum, however, the dichroism was greatly reduced at the higher temperature, indicating that the remaining features of the dichroism might well be associated with the *R* center.

To further verify this hypothesis, a comparison of six different runs shows that the stress-induced dichroism at large stresses (≈ 2 to 3 kg/mm^2) in the various regions of the spectrum was always in constant ratio from one part of the spectrum to another to within 30%, which is within the precision of the experiments as limited by the need for background subtractions or unreliable estimates of high optical densities. Included in this series was one crystal in which the *R* centers were first produced in high concentration (peak R_2 absorption constant 10 cm^{-1} at 2°K) and then thermally bleached at 100°C for 5 min to reduce the *R* concentration by a factor of 10. The stress-induced dichroism was reduced by this factor throughout the spectrum (except in the *F* region).

Polarized bleaching experiments similar to those of Okamoto[4] but over a 20:1 range of *R*-center concentrations have given further confirmation of the conclusions outlined below and are mentioned when pertinent. These conclusions are also consistent with the data obtained by Seidel *et al.*[11] on the temporary bleaching of the *R* center, which also show evidence of the R_1, R_2, R_M, and R_N absorptions.

Finally, in addition to identifying these various bands as transitions of the *R* center, the sign and magnitude of the dichroism are used in conjunction with the predictions of the previous section to determine the symmetries of the excited electronic states which correspond to these absorption bands. These conclusions are then compared with the qualitative predictions of Sec. IV. Unfortunately, interaction of the center with A_1 and A_2 symmetry vibration modes contributes most of the line broadening. Thus many of the effects of interaction with the E modes are obscured and it is difficult to push the comparison with the previous section in detail.

R_2 Band

The properties of the R_2 zero-phonon transition were of course the starting point of this whole program and the results of the work on the zero-phonon line of this transition were presented in an earlier section. This is also the band which shows the most marked stress-induced dichroism.

Figure 8 shows a plot of the ratio of intensities for light polarized in the [110] and [1$\bar{1}$0] directions in both the spike and the full absorption band at 2°K, with the stress applied along a [110] direction, as a function of the magnitude of that stress. Although the general appearance is that of a Langevin plot, the stress at which the dichroism reaches $1/\epsilon$ of its saturation value is much larger than that predicted from the stress coefficients (see Sec. III) and a temperature of 2°K. This is probably due to the presence of residual strains, in this instance of the order of 1 kg/mm^2, the limiting dichroism being achieved only when the applied stress is large compared with the random internal stresses. The value of 1 kg/mm^2 is comparable with that estimated by Sussman[19] from similar deviations from a Langevin curve observed by Känzig[20] for the O_2^- center in KCl. Although the limiting dichroism ratio for the R_2 broad band is difficult to estimate from the figure, it is approximately $\frac{1}{3}$, the value estimated theoretically for the limiting case of a large Jahn-Teller coupling. Estimates suggest that this ratio would be measurably less than $\frac{1}{3}$ for $k^2<1$ and hence this limiting dichroism, together with the earlier upper bounds placed on k^2, suggest that k^2 be limited by the bounds $1<k^2<7$.

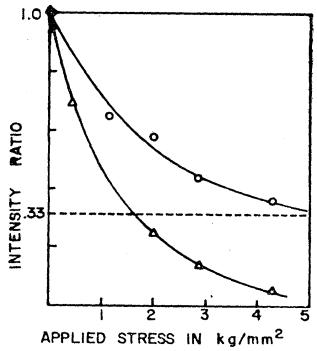

FIG. 8. Ratio of the absorption intensity of the *R* transition seen in (1$\bar{1}$0) light to that seen in (110) light for stress applied in the (110) direction and $T=2$°K. ○ the R_2 absorption band, Δ the R_2 zero-phonon line.

[19] J. A. Sussman, Physik Kondensierten. Materie **2**, 146 (1964).
[20] W. Känzig, J. Phys. Chem. Solids **23**, 479 (1962).

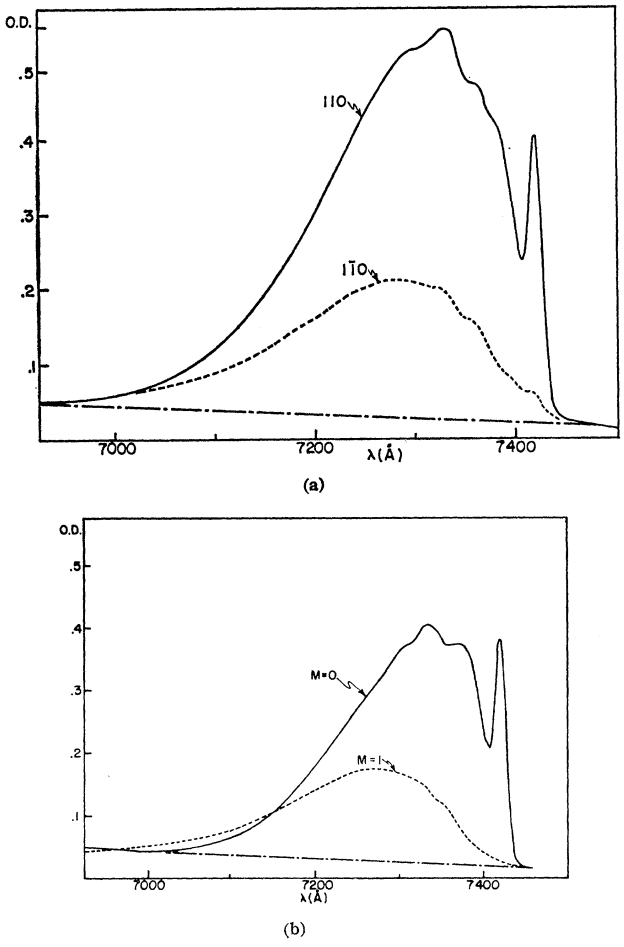

FIG. 9. R_2 dichroism at 2°K with applied 110 stress of 4 kg/mm². (a) —— Absorption in (110) light, - - - Absorption in (1$\bar{1}$0) light, —— Background assumed in correcting for Fig. B. (b) —— $M=0$ Absorption; Corrected (1$\bar{1}$0) spectrum - - - $M=1$ Absorption; (110) − (1$\bar{1}$0) spectrum.

Figure 9(a) shows the R_2 band in 110 and 1$\bar{1}$0 light with a [110] stress of 4 kg/mm². A slight residual zero phonon line, broadened by the instrumental resolution in this figure, is seen in [1$\bar{1}$0] light. This presumably results from the absorption by those centers where the residual internal stresses tilt the total stress away from the direction of the applied stress so that the incident [1$\bar{1}$0] light is not polarized perpendicular to the stress. One may correct the 1$\bar{1}$0 spectrum for this effect by subtracting enough of the 110 spectrum to cancel the residual zero phonon line, a procedure which gives the curve of Fig. 9(b) labeled $m=1$ transitions. According to the theory of Sec. VI, this spectrum is that to be associated with the excitation of an odd number of quanta in modes of E symmetry. By subtraction of this $m=1$ spectrum from the 110 spectrum one obtains the second curve of Fig. 9(b), corresponding to the transitions to the $m=0$ states which must involve an even number of E-mode quanta. It is tempting to use this data to try to distinquish between the effective density of modes, $N(\omega)$, of the modes of E and A symmetry which interact with the R center to broaden this absorption band. Unfortunately, the precision of the experiment does not warrant an attempt at such a separation in detail. The most prominent features of Fig. 9(b) are the presence of a shoulder in the $m=1$ spectrum at 0.014 eV with respect to the position of the zero-phonon line and the general shift of the centroid of the $m=1$ spectrum to higher energy by about 0.014 eV with respect to the $m=0$ band. If the shoulder is identified as a peak in the effective density of E modes in interaction with the center, the comparable shift in the centroid suggests that the mean number of E mode quanta involved in the broadening is not large, perhaps one or two, implying a $k^2 \approx 2$ to 4, consistent with the estimates above.

R_M Band

Figure 10 shows the [1$\bar{1}$0]-[110] difference spectrum under 110 stress in both KCl and KBr in the region of the M band and, for comparison, the spectrum in unpolarized light. The peak of the stress induced dichroism in KCl is displaced from the M peak by 130 Å and in KBr, the absorption band which gives rise to this dichroism is almost resolved from the M band. These results are consistent with the polarized bleaching experiment in which a strong dichroism is developed which again, in KCl, coincides in peak position with the band deduced from the stress dichroism.

The dichroism produced by polarized bleaching allows an estimate of the oscillator strength of the R_M transition relative to the R_2 and a comparison of this strength with the strength of the stress-induced dichroism indicates that the R_M, as the R_2, develops a dichroism ratio of about 3/1 with large stress.

The strength of the stress induced dichroism of the R_2 and R_M transitions implies that these transitions are from the ground electronic E states to excited A states. The fact that they show the opposite sign of dichroism implies that if one is A_1 the other must be A_2. The assignment of A_2 to the R_2 state and A_1 to the R_M state, the ordering opposite to that suggested by the Hirschfelder calculation, is based on estimates of the oscillator strength of these transitions. A molecular orbital picture predicts zero intensity for the transition to the A_1 state and the linear-combination-of-atomic-orbitals picture of Hirschfelder using only s orbitals on the individual centers predicts an A_2 to A_1 intensity ratio of 5 or 10, depending on the internuclear separation. States formed of linear combinations of nonionic configurations allowing excited p orbitals suggest equal oscillator strengths for the two transitions. Although none of these schemes is adequate, the weak A_1 oscillator strength predicted by the molecular orbital and the Hirschfelder calculation are the basis of the assignment of the R_2 as an A_2 transition and the R_M as an A_1.

This assignment of state symmetries agrees with a second aspect of Hirschfelder's calculations. The

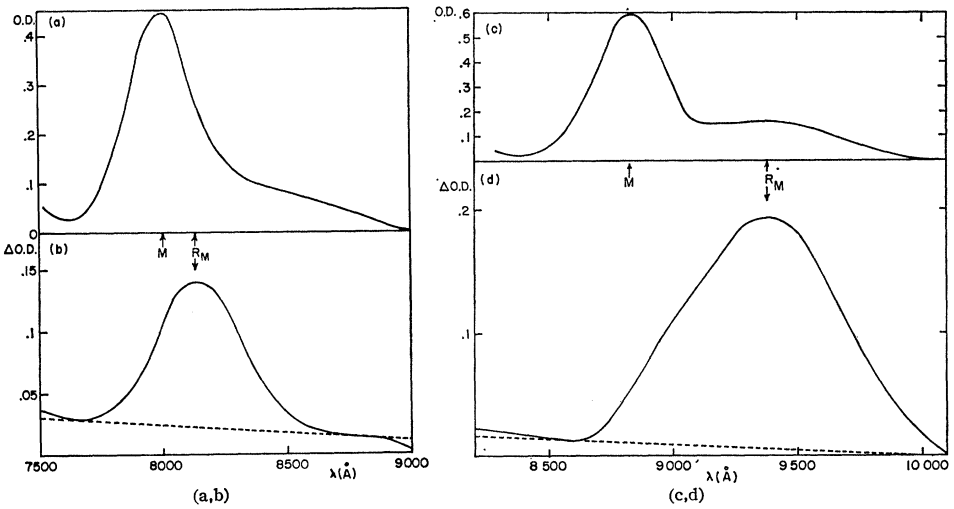

FIG. 10. The R_M band at 2°K. (a) The absorption in the M region of KCl. (b) $(1\bar{1}0)$-(110) spectrum in KCl with sufficient (110) stress to saturate the dichroism. The dashed line is the estimated base line. (c) The M region of KBr. (d) $(1\bar{1}0)$-(110) spectrum in KBr with (110) stress.

assumption that the R_2 state is of A_2 symmetry combined with the sign of the stress induced changes in the strength of the zero-phonon lines implies that a compressive stress along the defect's x axis must lower the state $\Psi_{y1\frac{1}{2}}$ since it is the transition in x light ($\Psi_{y1\frac{1}{2}} \rightarrow A_2$) which is enhanced by the stress. In computing the strain induced shift of the $\Psi_{y1\frac{1}{2}}$ state, the greatest contribution comes from the electronic state E_y, i.e., the sign of the splitting at the states $\Psi_{x1\frac{1}{2}}$ and $\Psi_{y1\frac{1}{2}}$ will be the same as for the states E_x and E_y. This result holds whether the Jahn-Teller coupling k is positive or negative. The assumption of the symmetry of the R_2 state as A_2 plus the zero-phonon line data thus imply that a compressive stress along the x axis must lower the energy of the E_y state relative to the E_x. But this is just the conclusion of Hirschfelder, namely that a distortion corresponding to a positive displacement of the Q_1 coordinate lowers the E_y state relative to the E_x. This observation also leads to the conclusion that the lower sheet of the Jahn-Teller potential surface does correspond as assumed earlier, to large $\mu(r)$, since in Eq. (7) it is the second terms for which $\Phi=0$ (positive Q_1) implies a favored electronic E_y state.

R_K Band

In the qualitative discussion of the excited states of the R center it was suggested that there should be additional transitions of the R center lying in and above the region of the F band. A very clear example of such a transition is a sharp band peaked at 4645 Å (see Fig. 7) which shows a dichroism relative to its total absorption comparable in strength to the R_2 or R_M. Since the dichroism is of the same sign as that of the R_2 band, this state must be of A_2 symmetry as well.

Okamoto[14] interpreted the dichroic spectra in this region in terms of two bands with dipole moments parallel to the 111 symmetry axis of the R center, one centered at 4340 Å and one at 5080 Å. Another interpretation of this data which would be consistent with the stress-induced dichroism might be that there is strong absorption in the F region associated with a dipole moment parallel to the defect axis. This would correspond to one-electron excitations on individual centers to p states lying perpendicular to the plane of the R center. A tail of this absorption extends to the violet side of the F band giving negative dichroism in the polarized bleaching experiment. Superimposed upon this tail is a positive dichroism associated with the R_K transition, centered at 4645 Å. This combination spectrum of a narrow positive band on the tail of a negative band then gives the appearance of having two negative peaks. This interpretation seems entirely consistent with data obtained from the polarized bleaching experiments of Okamoto and similar work carried out in conjunction with the experiments described here.

R_B Band

Between the R_1 and F bands there is a region which shows a marked dichroism under stress. A comparison of the magnitude of that dichroism with the total absorption in that region is suggestive of another A state, now with a very large breadth, and because of the breadth, appreciable oscillator strength. The sign of the dichroism implies that the state is of A_1 symmetry. This transition cannot be effectively studied by polarized bleaching because its effect is masked by the strong dichroism of the R transitions in the F region.

R_N Bands

In all of the stress experiments a weak dichroism was observed in the region of the N bands as illustrated in Fig. 11(b) and this dichroism was proportional to that observed in the regions of more obvious dichroism. These results implied the need to verify whether or not there is absorption of the R center in the N region.

In all of the samples showing R absorption there was also absorption in the N region and this absorption

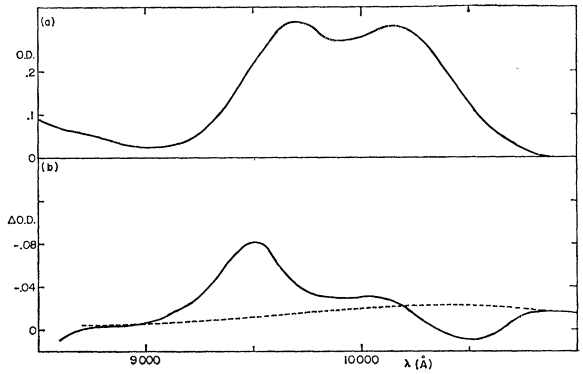

FIG. 11. The R_N band at 2°K. (a) The absorption in the N region of KCl. (b) $(1\bar{1}0)$-(110) spectrum with a (110) stress ≈ 3.5 kg/mm². The dashed base line is estimated from the stress dependence of the dichroism. The accuracy of the dichroic spectrum is ± 0.004.

consistently showed a doubly peaked structure. Similarly, orientation of the R center by polarized bleaching with R_1 light results in a double-peaked dichroism in the N region as found by Okamoto[4] and in similar experiments mentioned earlier. A number of runs with R concentrations varying over a range of 20:1 show that the intensity of the dichroism produced at 1.02 μ by polarized bleaching is consistently $0.17 \pm 30\%$ of the dichroism produced in the R_2 band. The dichroism in the other peak, at 0.96 μ does not stay in constant ratio to the R_2 dichroism but is never less than $0.20 \pm 30\%$. The variability of this ratio implies that there is another absorption in the N_1 region which does develop dichroism with bleaching by polarized light but the lower bound on the ratio suggests that part of the N_1 absorption is to be associated with a transition of the R center. A review of many runs, looking simply at the ratios of N_1 (0.96 μ), N_2(1.02 μ) to the R_2 absorption shows that the ratios are never less than 0.20 and 0.16, respectively, within the precision limited by the significance of base line estimates, about 30%. In both cases, the ratio is frequently more than these values indicating that there are several centers giving absorption in the general region of the N bands. Thus the conventional absorption and polarized bleaching experiment indicate, though not conclusively, that there is absorption of the R center in the region of the N_1 and N_2 bands. Compton and Schnatterly[5] in a study in the radiation equilibrium among defects in KCl, have presented data indicating that neither the N_1 nor the N_2 absorption is linearly proportional to the R_2 absorption. There is considerable evidence that a number of distinct absorption bands occur in the N region and thermal bleaching (at 100°C) of the R center reveals absorption bands overlapping the usual R_1 and R_2 bands. If there are several centers contributing to both the R and N absorption bands it is difficult to draw positive conclusions from the work of Compton and Schnatterly. For lack of compelling experimental arguments against the hypothesis, the stress-induced dichroism in the N bands will be assumed to arise from the R center and will be denoted as the R_N doublet.

The presence of the doublet structure of the R_N band and the qualitative behavior of the stress induced dichroism both imply that the R_N band should be assigned to an $E \rightarrow E$ electronic transitions. The stress induced dichroism is compared in Fig. 11 with the shape of the normal R_N absorption. The qualitative behavior is similar to that predicted in the previous section for the admixture of $l=\frac{5}{2}$ states into the $l=\frac{1}{2}$ state by a trigonal term in the Jahn-Teller potential; the transitions to the upper and lower sheets of the excited state surface show dichroism of opposite sign. The magnitude of the dichroism indicates an admixture of 10–20% of $l=\frac{5}{2}$ state into the ground state. The sign of the dichroism of the $E \rightarrow E$ transitions depends both upon the sign of the "trigonal potential" and upon the sign of the linear Jahn-Teller coupling in the excited states. Preference of the system for values of $\phi = 0 \bmod \frac{2}{3}\pi$ would require the R_N and R_1 states to have a Jahn-Teller coupling opposite in sign to that of the ground state. Assuming the same sign of coupling for all three states, the data implies that the more stable distortions correspond to $\phi = \frac{1}{3}\pi \bmod \frac{2}{3}\pi$.

It is gratifying that the Hirschfelder calculation gives an E state lying below the A_2 and A_1 states already assigned to the R_2 and R_M transitions; the R_N doublet is naturally identified with this lowest excited E state.

R_1 Band

The R_1 band has long been assumed to be associated with the same center as the R_2 band; it is not surprising then that it shows a stress-induced dichroism as illustrated in Fig. 12. The weakness of the dichroism, comparable to that of the R_N band if normalized to the band height, indicates that the R_1 is also an $E \rightarrow E$ transition. The shape of the dichroism does not follow

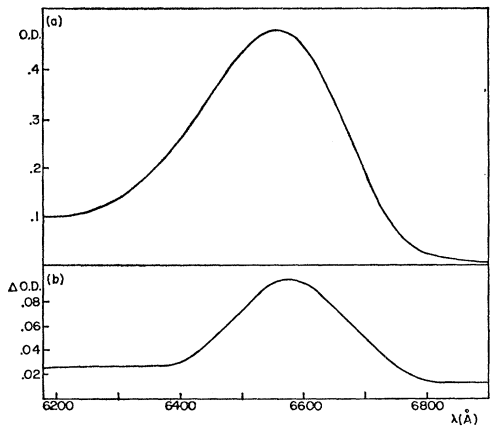

FIG. 12. The R_1 band at 2°K. (a) The R_1 absorption in KCl. (b) $(1\bar{1}0)$-(110) spectrum with a stress of ≈ 2 kg/mm².

the shape of the absorption band but cuts off sharply on the short-wavelength side of the band. Also, the R_1 does not show the doublet structure of the R_N band. The probable source of this difference is that this state shows a weaker Jahn-Teller effect than do the R_N and ground states. A smaller splitting would then not be resolved but the tendency for opposite sign of dichroism of the two components of the R_N is reflected in the R_1 by the sharp reduction of the dichroism on the violet side of the band when compared with the shape of the R_1 absorption. Another possibility which cannot be ruled out is that the R_1 Jahn-Teller splitting is larger than the R_N and the other component of the doublet lies under the F band. If the dichroism of this upper component were weak it could have been masked by the uncertainties in subtracting the contribution to the dichroism of the strain splitting of the F excited state. A small Jahn-Teller effect seems the more likely explanation.

R Luminescence

Some rather crude luminescence experiments were also performed to see if they would shed any further light on the R-center level structure. In particular it was important to determine whether the luminescence at 4°K would show a splitting similar to the R_N absorption. Figure 13 shows the emission spectrum for excitation at 6600 Å with an exciting bandwidth of 400 Å; on the same plot is shown the R_N absorption spectrum. A simple configuration coordinate picture implies that if the R emission is from the R_N state to the ground state and if the curvatures of the potential in the two states are the same, the absorption and emission splittings are the same. The absence of an observable splitting is disappointing but only a small additional broadening at the emission would prevent resolution of the doublet structure. The asymmetry of the emission suggests that the lower energy component is weaker than the higher. If a Stokes shift is predicted on the basis of the breadth of the components of the R_N absorption and the most naive configuration coordinate diagram, the results are consistent with the observed

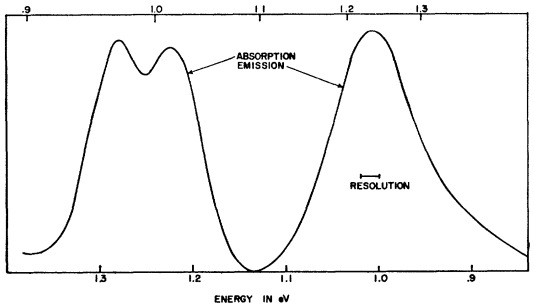

FIG. 13. The emission spectrum of KCl containing R centers at 4.2°K with excitation in the R_1 band, 6400-6800 Å. The absorption spectrum of the N bands, most of which is due to the R_N absorption, is shown for comparison.

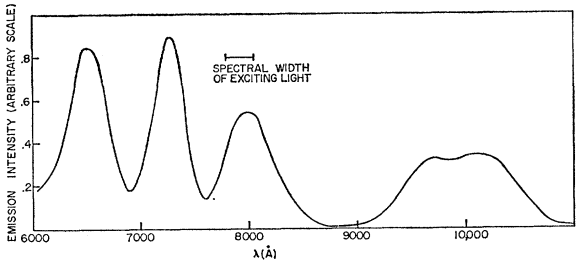

FIG. 14. R-center luminescence excitation spectrum. The emission intensity at 1.21μ is plotted as a function of the wavelength of the exciting light. The results have not been corrected for the wavelength dependence of the intensity of the incident light nor for attenuation of the incident light by the central and hence are only of qualitative significance.

shift. An additional piece of evidence is the values of the correlation in polarized luminescence experiments,[1,3] $P_{110}=20$–25%, $P_{100}\approx 0\%$. The analysis of this experiment by van Doorn[1] shows that these results are predicted if the luminescents transition moment lies in the plane of the triangle, consistent with the assignment of the R_N state as the initial state.

Figure 14 shows an excitation spectrum for emission at 1.2 μ. It has no quantitative significance since it is not normalized to constant incident flux nor is it corrected for the high optical density in the R absorption bands. It does show qualitatively, however, that excitation of the R luminescence is possible in at least four of the R transitions discussed above, the R_1, R_2, R_M, and R_N.

Application of uniaxial stress to the crystal did not give an observable dichroism in emission. Dichroism in emission would result from trigonal mixing of the $l=\frac{1}{2}$ and $l=\frac{5}{2}$ states of the R_N system rather than of the ground system and if that mixing in the R_N levels were $<\frac{1}{3}$ of that of the ground state, the experiment would not have had sufficient sensitivity to detect the dichroism.

Although the evidence, other than the theoretical simplicity, is not strong, the initial state for the R luminescence is assigned to the R_N state which may be populated by direct excitation in the R_N band or by radiationless transitions from the higher excited states of the center.

Summary

Table III lists the various absorption bands of the R center, their symmetry, peak position, half-widths and oscillator strengths as deduced from the data from both the stress induced dichroism and polarized bleaching experiments. These bands represent those R transitions which show easily measurable stress-induced dichroism. If the R center had the full symmetry of the H_3 model (D_{3h}) the states would be either even or odd in reflection in the plane of the triangle of vacancies and the selection rules would be as indicated in Fig. 3. These selection rules should be approximately valid for the R center with C_{3v} symmetry. The stress induced dichroism is sensitive only to those transitions with

TABLE III. Summary of the stress-sensitive R-center absorption bands.

Electronic band	symmetry	Peak (Å)	Width Å	Width eV	Peak relative to R_2[b] Absorption[c]	Stress[d]	Polarized bleaching[e]	Relative oscillator strength
R_K	A_2	4645±10	155±10	0.089	0.10	0.11		0.18
R_B	A_1	6200±150	1200±150	0.4	0.09	0.075	(0.1)	0.65
R_1	E	6550±10	270±10	0.078	0.75		0.8	1.2
R_2	A_2	7310±20	220±20	0.051	1	1	1	1.0
R_M	A_1	8140±10	390±10	0.073		0.20	0.21	0.29
R_N	E	9680±50 10 170±50	470±50 550±50	0.062 0.065 [a]	<0.18		0.15	0.37

[a] The decomposition of this absorption into two bands is rather arbitrary both because of the absence of a detailed theory for such an $E-E$ doublet and because of the probable contribution of other centers to the absorption in this spectral region.
[b] Accuracy: 20% for the R_K, R_B, and R_N and 10% for the R_1 and R_M.
[c] The R_M is masked by the M absorption.
[d] The magnitude of the R_1 and R_N stress-induced dichroism does not give the oscillator strengths of these bands.
[e] The background dichroism due to the R_F transition is too large to allow a reliable estimate of the R_K and R_B oscillator strengths.

transverse moments and one should expect to see no temperature-dependent stress dichroism induced in the absorption bands with moments perpendicular to the plane of the triangle. The fact that Okamoto observes strong polarized bleaching in the F region, of opposite sign to that elsewhere in the spectra, confirms the assignment of the odd parity excitations to the general region of the F band. Thus one has accounted experimentally for all of the qualitatively predicted observable transitions of Fig. 3 except the upper two E states. If their oscillator strength (or breadth) were comparable with that of the R_K(or R_B) bands the stress-induced dichroism would be too weak to observe. One should also recognize, of course, that the scheme of Fig. 3 is based on very simple arguments and must not be interpreted literally, particularly for the higher excited states.

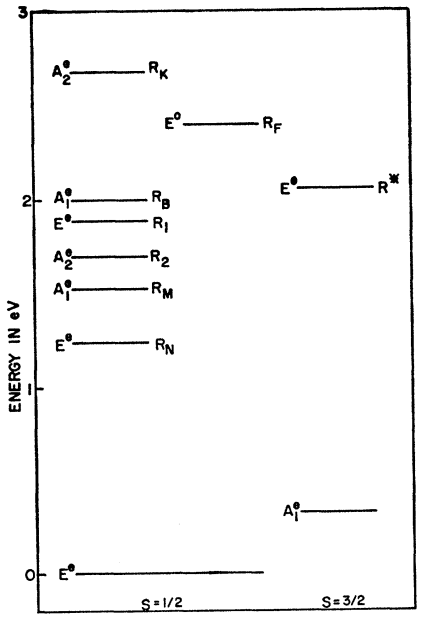

FIG. 15. Proposed energy-level diagram for the R center in KCl. The states on the left are identified by the stress-induced dichroism. The R_F state is observed by Okamoto (Ref. 4) in polarized bleaching experiments. The position of the lowest spin quartet is estimated from the Hirschfelder calculation, and the excited spin quartet from the experiments of Seidel (Ref. 11).

VIII. CONCLUSION

The data on the stress splitting of the zero-phonon line imply unequivocally that this absorption results from a transition from a doubly degenerate ground state to a singlet excited state, the degeneracy of the ground state resulting from the presence of a 111 axis of symmetry for the defect in question. The model of van Doorn of the R center as a cluster of three F centers predicts both the 111 symmetry axis and the degeneracy of the ground state.

Qualitative arguments allow the prediction that the R center should have a number of optically accessible excited states. Because of the preferential population of the lower component of the strain split ground state at low temperatures, all of the states accessible by dipole transitions with electric field polarized in the plane of the F_3 triangle should show a stress-induced dichroism. The qualitative features of the dichroic spectrum are satisfactorily interpreted in terms of the electronic states suggested in analogy with calculations of the H_3 molecule as modified by the dynamic Jahn-Teller effect.

These experiments are interpreted to give the energies and symmetries for 6 of the excited states of the R center, the lowest four being in reasonable agreement with the continuum approximation for the F_3 model. An additional state, or perhaps an unresolved pair of states, with transition moment perpendicular to the plane of the triangle is observed in polarized bleaching experiments by Okamoto.[4] The calculation of Sec. IV suggests that the spin quartet state observed by Seidel *et al.*[11] lies $\frac{1}{3}$ eV above the ground state. Finally, the results of the temporary bleaching experiments of Seidel *et al.*[11] give the location of at least one of the

higher spin-quartet states relative to the lowest spin quartet. This excited state is probably the lower quartet E^e of Fig. 3, though this symmetry assignment has not been confirmed experimentally. Figure 15 gives a proposed energy-level diagram for the R center in KCl, using the results noted above.

ACKNOWLEDGMENTS

I should like to thank D. C. Krupka and R. A. Herendeen for assistance with the experiments. The measurement of the hydrostatic pressure shift by D. B. Fitchen was most useful in estimating the reliability of the stress measurements.

PHYSICAL REVIEW VOLUME 138, NUMBER 1A 5 APRIL 1965

Optical Properties of Graphite*

E. A. Taft and H. R. Philipp
General Electric Research Laboratory, Schenectady, New York
(Received 2 November 1964)

The complex dielectric constant $\epsilon(\omega)=\epsilon_1+i\epsilon_2$ and associated functions are derived by application of the Kramers-Kronig relation to reflectance data for graphite obtained in the energy range to 26 eV. It is possible to divide the optical properties into two spectral regions. In the range 0 to 9 eV, intra- and interband transitions involve mainly the π bands. At higher energies, a broad absorption peak near 15 eV is associated with interband transitions involving the 3 σ electrons per atom. This viewpoint is strongly supported by evaluation of the sum rules for n_{eff}. Plasma resonances which produce peaks in the energy-loss function $-\text{Im}\epsilon^{-1}$ at 7 and 25 eV are identified and described physically. At low energies, structure in the reflectance curve near 0.8 eV is attributed to the onset of transitions between the E_2 and E_3 bands at the point K. This yields a value for γ_1 of $\approx$0.4 eV.

I. INTRODUCTION

In recent years the study of graphite has received much attention in the literature. This crystal exhibits unique electronic properties of interest to the theoretical, as well as the experimental physicist. It is possible to observe a number of phenomena, for example; the de Haas-Van Alphen effect, magnetoreflection and resistance effects, cyclotron resonance, diamagnetic susceptibility, and so forth, which yield direct information about the Fermi surface. Theoretical work has progressed at a similar pace, and today the electronic structure of graphite for energies near the Fermi energy is well understood.[1,2]

Optical studies yield additional information, principally about excited electronic states of the crystal. In particular, they concern effects which can be described most conveniently in terms of the frequency-dependent dielectric constant. Experimentally, the complex dielectric constant can be evaluated over an extended energy range by the well-known Kramers-Kronig analysis of reflectance data,[3] a procedure which has been employed in a number of such studies to date.[4]

The main feature of the reflectance spectrum of graphite is a sharp minimum in the curve which occurs at about 8 eV. Near this energy the crystal becomes relatively transparent, and it is possible to separate, quite unambiguously, the dielectric constants associated with strong absorption processes at higher and at lower energies. For the purposes of further analysis, it is convenient to divide the optical properties of graphite into two spectral regions. In the energy range 0 to 9 eV, intra- and interband optical transitions involve mainly the π bands which arise from the one electron per atom, atomic $2p_z$ orbitals, extending above and below the carbon-layer planes which make up the graphite crystal. It is these electrons which play the principal role in the electrical conductivity. At higher energies, a broad peak of optical absorption near 15 eV is associated with interband transitions involving the 3 σ electrons per atom, which form the coplanar bonds joining one carbon to its three neighbors within the layer. This viewpoint is supported by evaluation of the sum rule for the effective number of electrons which has been used in previous work[4,5] to indicate the distribution of oscillator strengths for transitions from the valence bands. For graphite, this integral saturates near one electron per atom just above 8 eV and again near four electrons per atom at the plasma frequency $\hbar\omega_p$, $\approx$25 eV where the total oscillator strength for transitions involving the combined π and σ bands is essentially exhausted.

Two peaks are observed in the energy-loss function,

* This work was reported in part at the Philadelphia Meeting of the American Physical Society [H. R. Philipp, Bull. Am. Phys. Soc. 9, 211 (1964)].

[1] For a review of this work see R. R. Haering and S. Mrozowski, *Progress in Semiconductors* (John Wiley & Sons, Inc., New York, 1960), Vol. 5, p. 273.

[2] M. S. Dresselhaus and J. G. Mavroides, IBM J. Res. Develop. 8, 262 (1964); Carbon 1, 263 (1964).

[3] H. R. Philipp and E. A. Taft, Phys. Rev. 113, 1002 (1959).

[4] See, for example, H. Ehrenreich, H. R. Philipp, and B. Segall, Phys. Rev. 132, 1918 (1963).

[5] H. R. Philipp and H. Ehrenreich, Phys. Rev. 129, 1550 (1963).